

Supplementary Information

Crystal Structures and Luminescent Properties Of A D-A type CIEgen and Its Zn(II) Complexes

Jian-Biao Song^a, Gui-lei Liu^{*b}, Liang Hao^a, Fang Zhang^c and Hui Li^{*a}

^a Key Laboratory of Clusters Science of Ministry of Education, School of Chemistry and Chemical Engineering, Beijing Institute of Technology, Beijing, 100081, P.R. China.
E-mail: lihui@bit.edu.cn; Fax: +86 10 68912667

^b National Research Center for Geoanalysis, P.R.China.
E-mail: liuguilei2008@163.com

^c Analysis and Testing Center, Beijing Institute of Technology, Beijing, 100081, P.R.China.
E-mail: 00258104@bit.edu.cn

Content

1. Infrared Radiation spectrum of CIE-C and CIE-P	3
2. ^1H NMR and ^{13}C NMR spectrums of CIE-C in DMSO- d_6	4
3. ^1H NMR and ^{13}C NMR spectrums of CIE-P in DMSO- d_6	5
4. ^1H NMR and ^{13}C NMR spectrums of complex 1 in DMSO- d_6	6
5. ^1H NMR and ^{13}C NMR spectrums of complex 2 in DMSO- d_6	7
6. Thermal gravity analysis of CIE-C and CIE-P	8
7. Thermal gravity analysis of complexes 1 and 2	8
8. X-ray powder diffraction of CIE-C and CIE-P	9
9. Selected bond distances (\AA) and angles ($^\circ$) for CIE-C , complexes 1 and 2	10
10. X-ray powder diffraction of complexes 1 and 2	12
11. Scanning electron microscope of smashed CIE-C and CIE-P	13
12. Solid state fluorescent spectra of CIE-C , CIE-P and CIE-Powder soaking with different kinds of solutions.....	14
13. X-ray powder diffraction of CIE-C , CIE-P and CIE-Powder soaking with different kinds of solutions..	14
14. Selected H-bonding distances of CIE-C , CIE-P , complexes 1 and 2	15
15. Investigation of AIE property of CIE-C	16
16. Bar graph of solid state maximum fluorescent spectra of CIE-C , CIE-P , complexes 1 and 2	17
17. Fluorescence spectra of 1 in different kinds of solutions and of methanol-tetrahydrofuran mixtures with different ratios.....	18
18. Fluorescence spectra of 2 in different kinds of solutions and of methanol-tetrahydrofuran mixtures with different ratios.....	19
19. UV-Vis spectra of complexes 1 and 2 in different kinds of solutions.....	20
20. UV-Vis titration of complexes 1 and 2 with pyrazine and 4,4'-bipyridine.....	21
21. Comparison of fluorescence spectra of CIE-C , complexes 1 and 2 in THF.....	22

1. Infrared Radiation spectrum of **CIE-C** and **CIE-P**

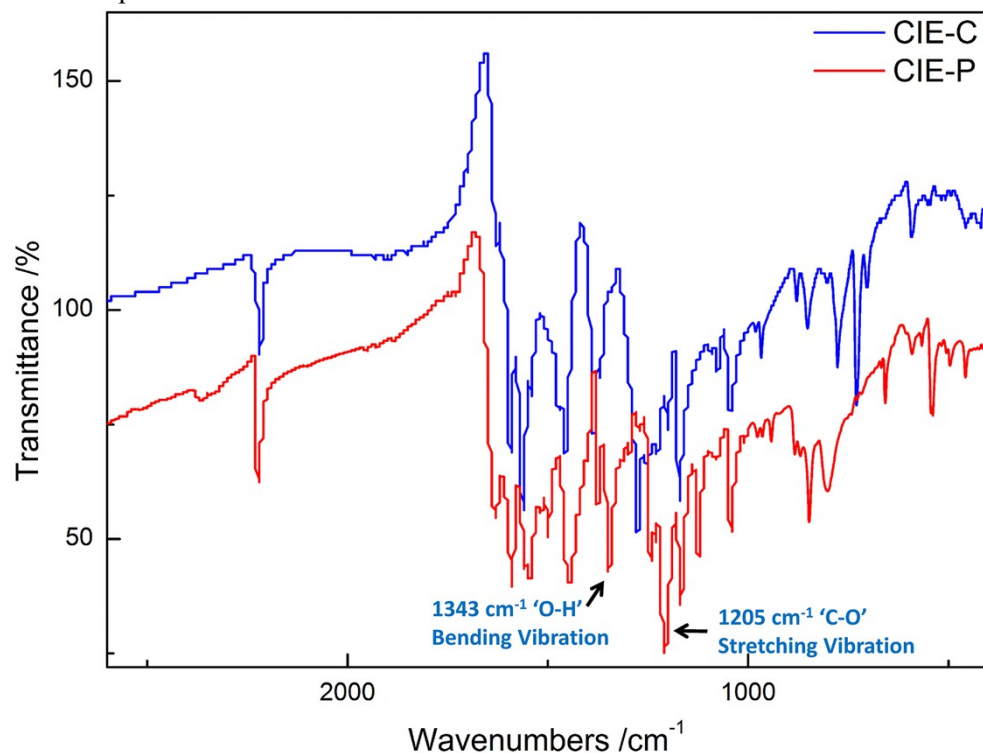


Fig. S1 IR spectrum of **CIE-C** and **CIE-P**.

2. ^1H NMR and ^{13}C NMR spectra of **CIE-C** in $\text{DMSO}-d_6$

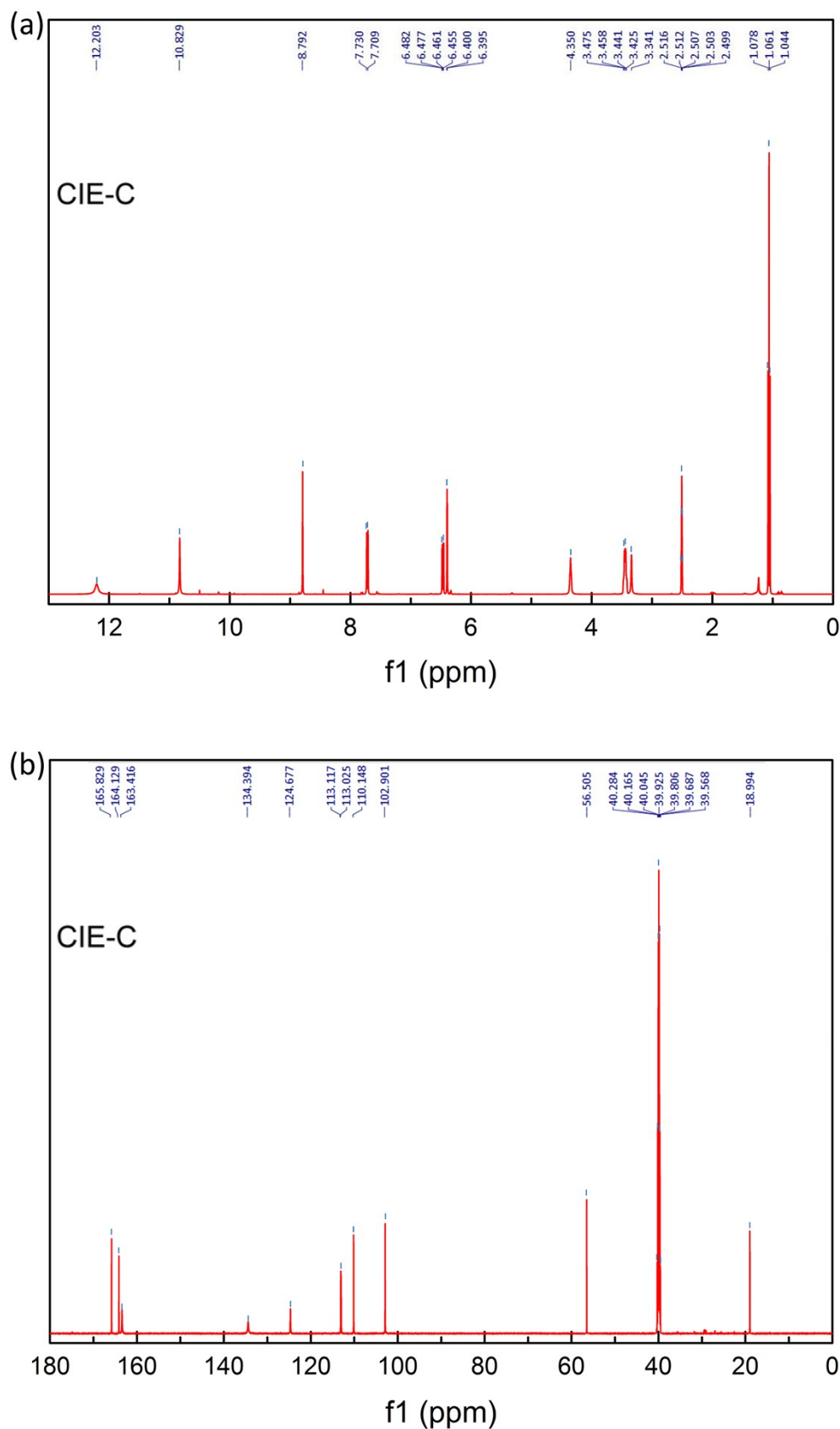


Fig. S2 ^1H NMR(a) and ^{13}C NMR(b) spectrums (400 MHz, 298K) of **CIE-C** in $\text{DMSO}-d_6$.

3. ^1H NMR and ^{13}C NMR spectra of **CIE-P** in $\text{DMSO}-d_6$

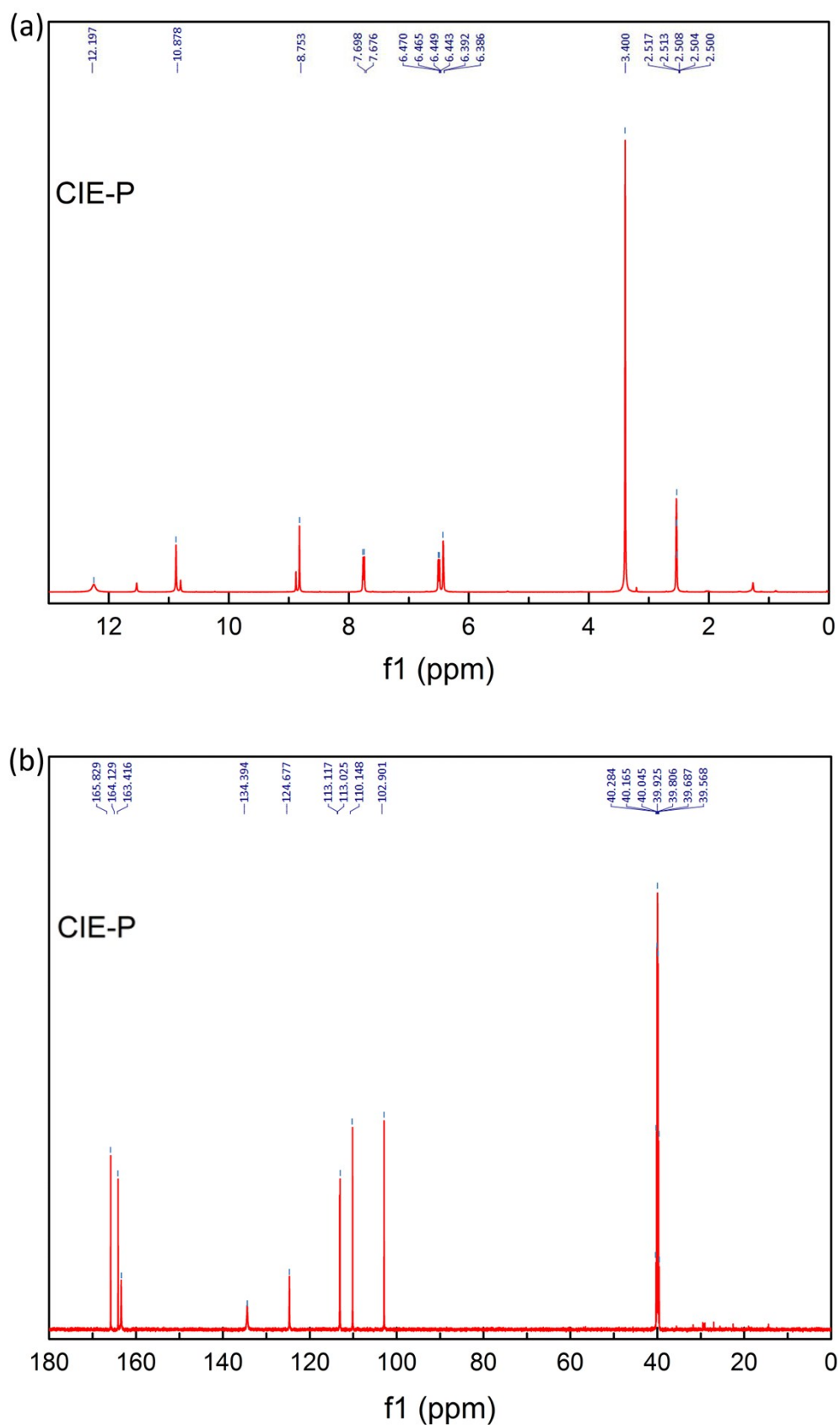


Fig. S3 ^1H NMR(a) and ^{13}C NMR(b) spectrums (400 MHz, 298K) of **CIE-P** in $\text{DMSO}-d_6$

4. ^1H NMR and ^{13}C NMR spectra of complexes **1** in $\text{DMSO}-d_6$

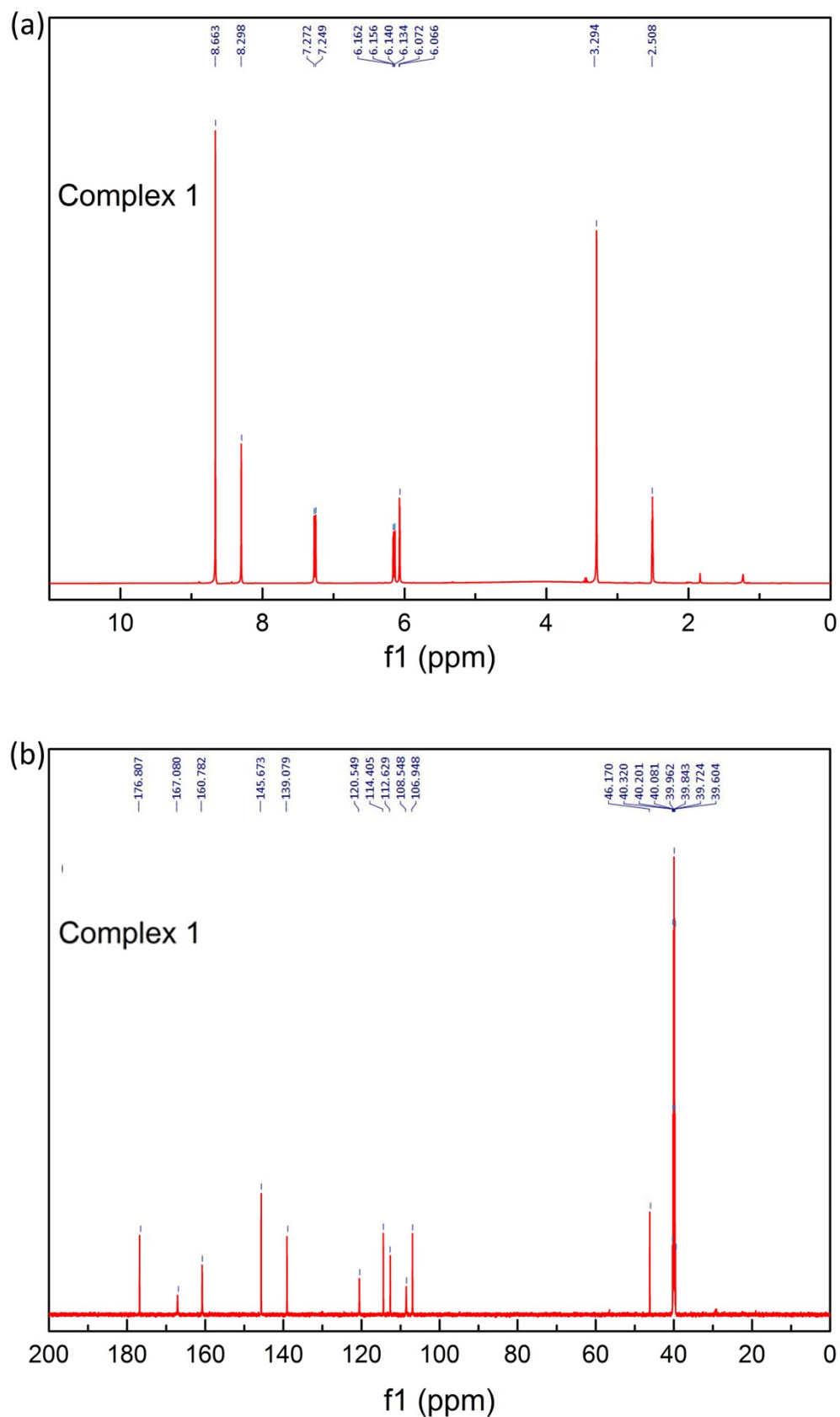


Fig. S4 ^1H NMR(a) and ^{13}C NMR(b) spectra (400 MHz, 298K) of complexes **1** in $\text{DMSO}-d_6$.

5. ^1H NMR and ^{13}C NMR spectra of complexes **2** in $\text{DMSO}-d_6$

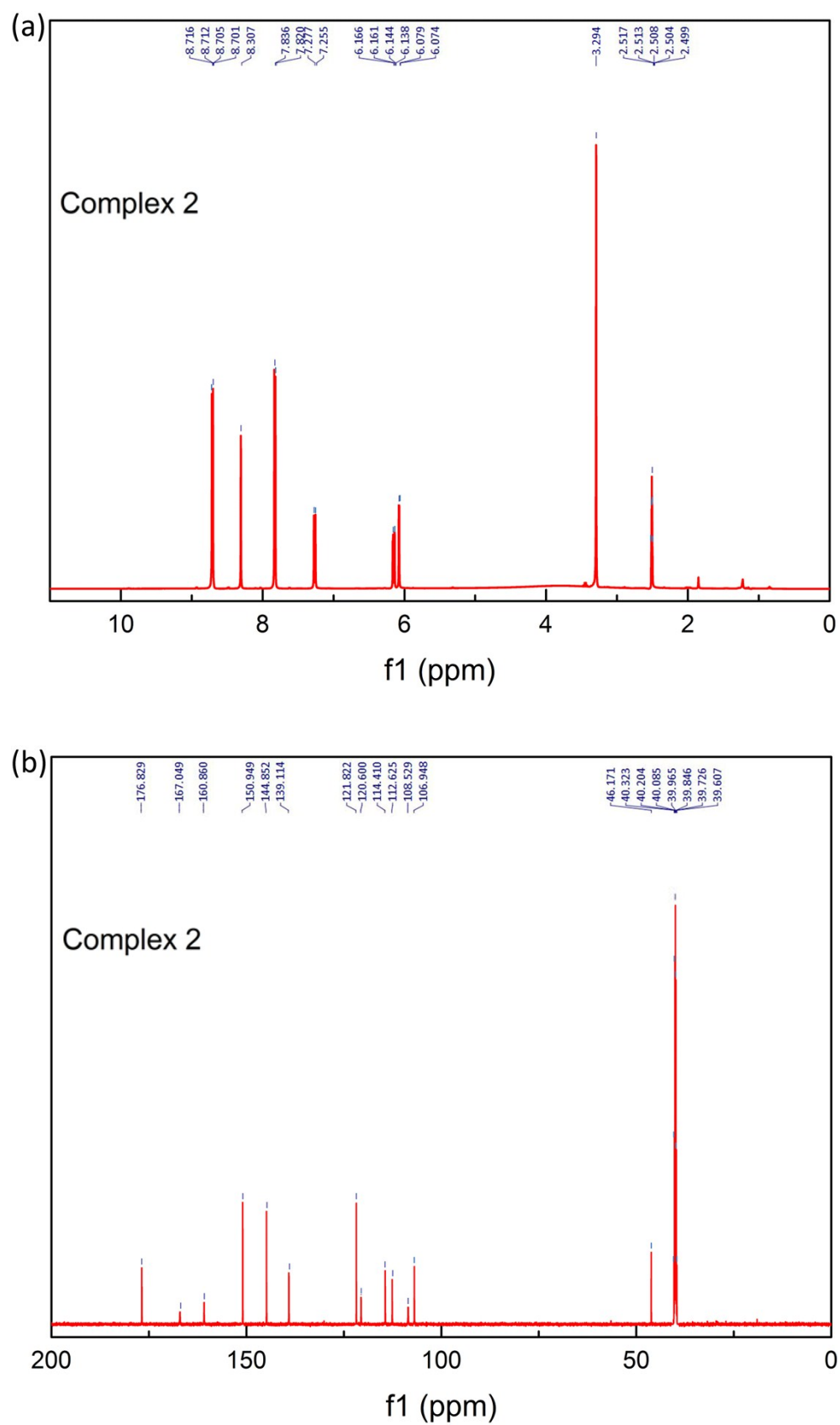


Fig. S5 ^1H NMR(a) and ^{13}C NMR(b) spectra (400 MHz, 298K) of **2** in $\text{DMSO}-d_6$.

6. Thermal gravity analysis of CIE-C and CIE-P

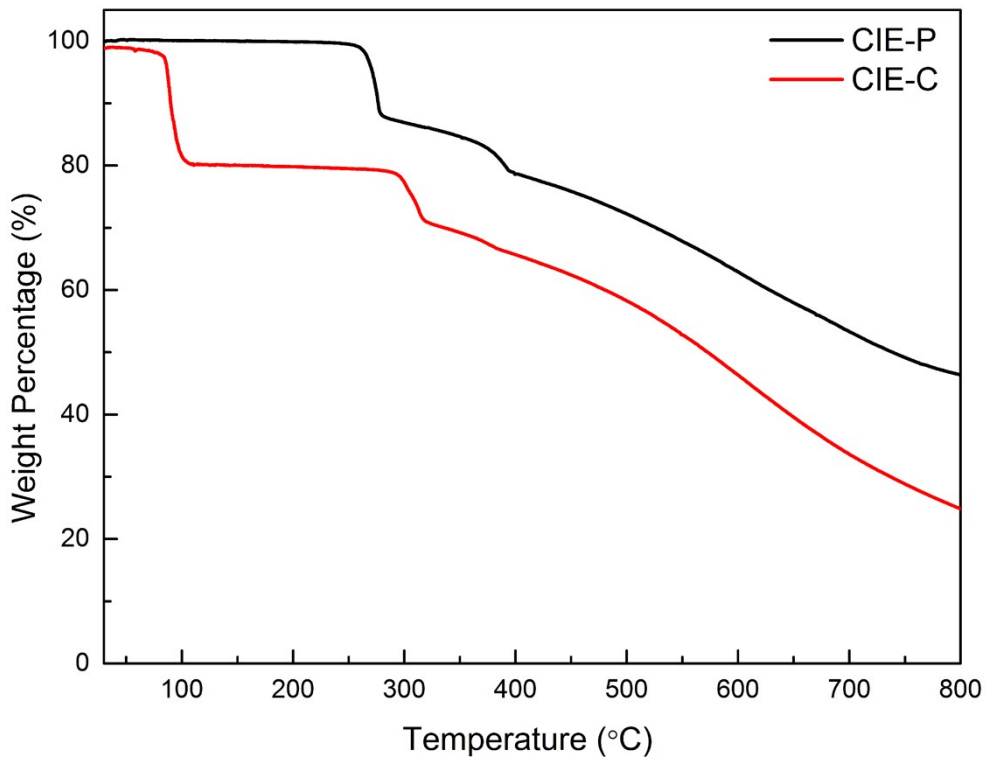


Fig. S6 TGA curves of CIE-C and CIE-P.

7. Thermal gravity analysis of complexes 1 and 2

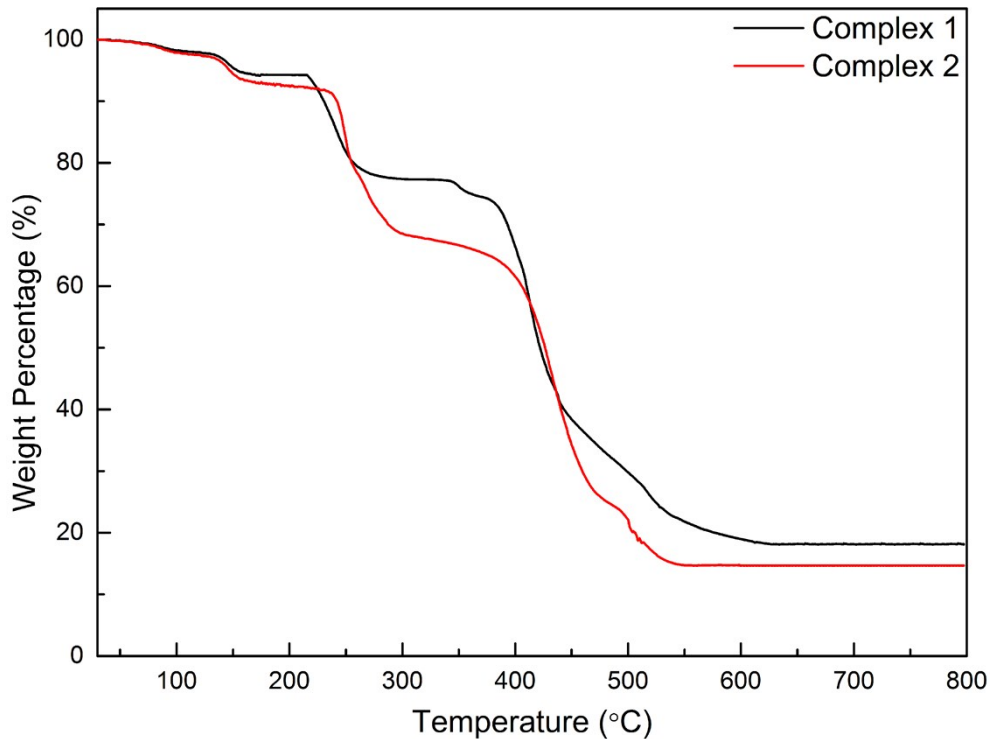


Fig. S7 TGA curves of 1 and 2.

8. X-ray powder diffraction of **CIE-C** and **CIE-P**

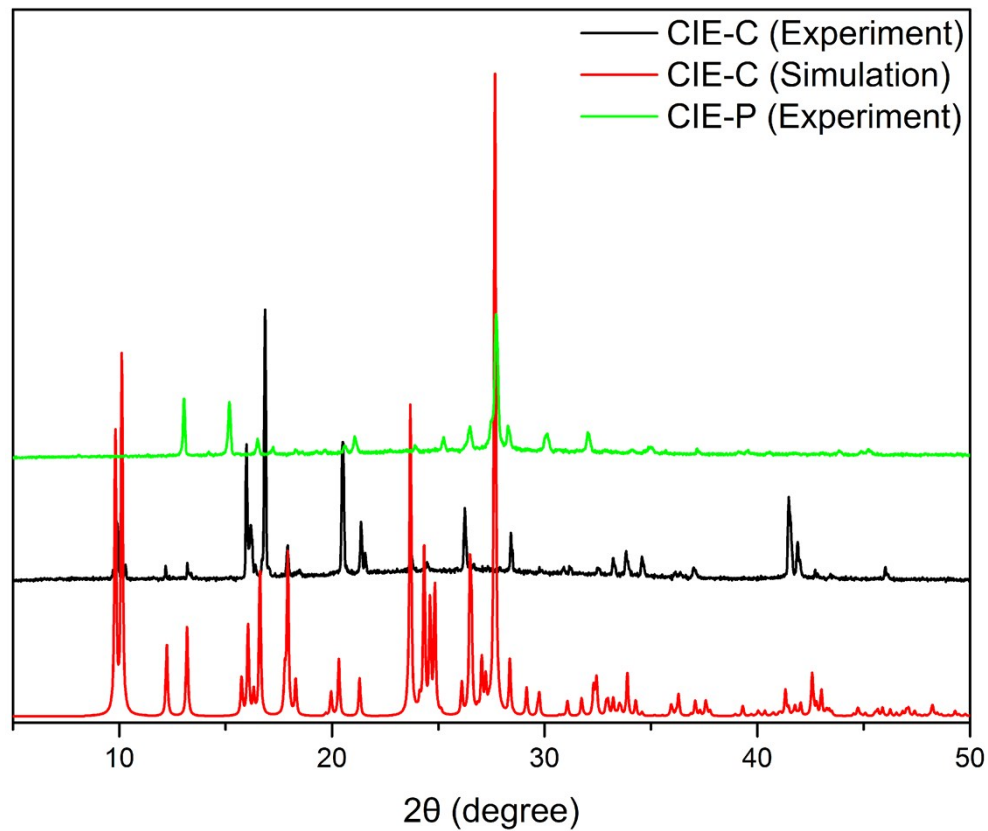


Fig. S8 PXRD patterns show the comparison between the experimental value and calculated ones for **CIE-C** and **CIE-P**.

9. Selected bond distances (\AA) and angles ($^\circ$) for **CIE-C**, complexes **1** and **2**

Table S1. Selected bond distances (\AA) and angles ($^\circ$) for **CIE-C**.

O3—C11	1.393 (4)	C3—C4	1.429 (3)
C10—C11	1.439 (4)	N1—C1	1.137 (3)
O1—C9	1.347 (2)	C7—C8	1.386 (3)
C6—C5	1.370 (3)	C7—C6	1.400 (3)
O2—C7	1.345 (2)	C9—C8	1.383 (3)
N2—C3	1.303 (2)	C9—C4	1.414 (3)
N2—C2	1.377 (2)	C4—C5	1.411 (3)
C2—C2i	1.371 (4)	C2—C1	1.443 (3)
C3—N2—C2	120.61 (16)	C9—C8—C7	120.17 (19)
C2i—C2—N2	121.43 (10)	C5—C6—C7	119.17 (18)
C2i—C2—C1	118.73 (11)	C6—C5—C4	121.89 (19)
N2—C2—C1	119.84 (16)	O3—C11—C10	114.5 (3)
N2—C3—C4	122.00 (17)	C8—C9—C4	120.54 (18)
O2—C7—C8	122.59 (19)	C5—C4—C9	117.68 (18)
O2—C7—C6	116.86 (18)	C5—C4—C3	120.31 (18)
C8—C7—C6	120.55 (18)	C9—C4—C3	122.00 (17)
O1—C9—C8	117.85 (17)	N1—C1—C2	176.0 (2)
O1—C9—C4	121.61 (17)		

Symmetry codes: (i) $-x+1, y, -z+1/2$.

Table S2. Selected bond distances (\AA) and angles ($^\circ$) for **1**

Zn1—O1	1.9528 (13)	O1—Zn1—N5	106.31 (6)
Zn1—O2	1.9679 (12)	O2—Zn1—N5	98.79 (6)
Zn1—N1	2.0769 (14)	N1—Zn1—N5	99.15 (6)
Zn1—N2	2.1118 (14)	N2—Zn1—N5	96.21 (6)
Zn1—N5	2.1418 (15)	C8—O2—Zn1	130.55 (10)
O1—Zn1—O2	95.98 (5)	C19—O1—Zn1	129.39 (11)
O1—Zn1—N1	89.28 (5)	C15—N1—C9	122.70 (14)
O2—Zn1—N1	159.05 (6)	C15—N1—Zn1	124.88 (12)
O1—Zn1—N2	156.10 (6)	C9—N1—Zn1	112.11 (11)
O2—Zn1—N2	88.23 (5)	C18—N2—Zn1	125.58 (11)
N1—Zn1—N2	79.17 (5)	C14—N2—Zn1	110.89 (11)
C33—N5—Zn1	120.73 (12)	C25—N5—Zn1	122.76 (12)

Table S3. Selected bond distances (\AA) and angles ($^\circ$) for **2**

N3—Zn1	2.107 (2)	C19—N5—Zn1	123.28 (16)
N4—Zn1	2.096 (2)	C27—N6—C26	115.8 (3)
N5—Zn1	2.085 (2)	C11—O1—Zn1	131.06 (16)
O1—Zn1	1.9823 (17)	C18—O2—Zn1	127.50 (16)
O2—Zn1	1.9513 (17)	O2—Zn1—O1	97.58 (7)
C5—N3—Zn1	126.62 (16)	O2—Zn1—N5	104.05 (8)
C3—N3—Zn1	111.50 (16)	O1—Zn1—N5	97.76 (8)
C12—N4—C4	122.5 (2)	O2—Zn1—N4	88.77 (8)
C12—N4—Zn1	124.95 (18)	O1—Zn1—N4	160.69 (8)
C4—N4—Zn1	112.24 (16)	N5—Zn1—N4	98.35 (8)
C23—N5—C19	117.1 (2)	O2—Zn1—N3	153.10 (8)
C23—N5—Zn1	119.48 (16)	O1—Zn1—N3	88.00 (8)
N5—Zn1—N3	101.20 (8)	N4—Zn1—N3	78.48 (8)

10. X-ray powder diffraction of complexes **1 and **2****

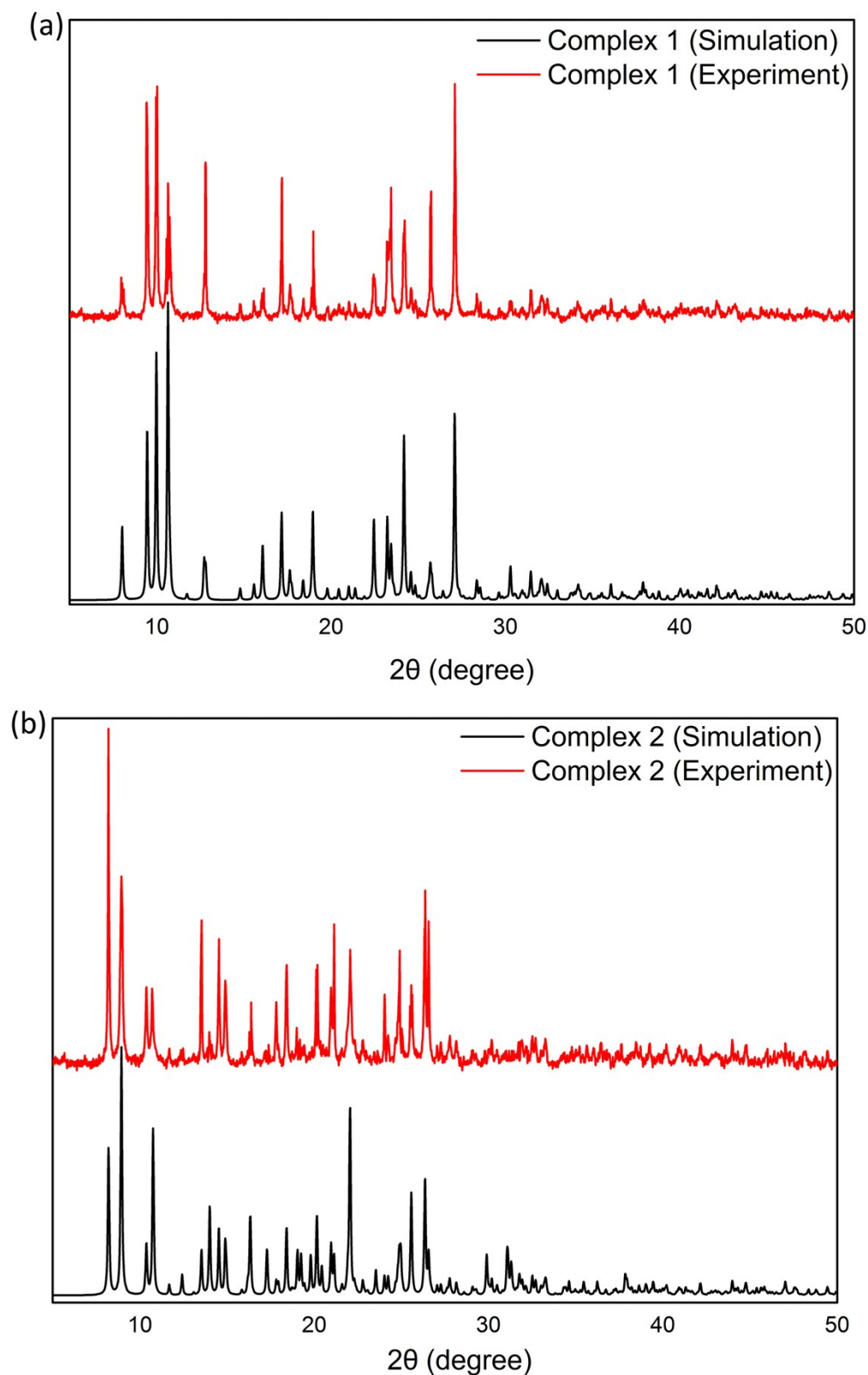


Fig. S9 PXRD patterns show the comparison between the experimental value and calculated ones for complexes **1** (a) and **2** (b).

11. Scanning electron microscope of smashed **CIE-C** and **CIE-P**

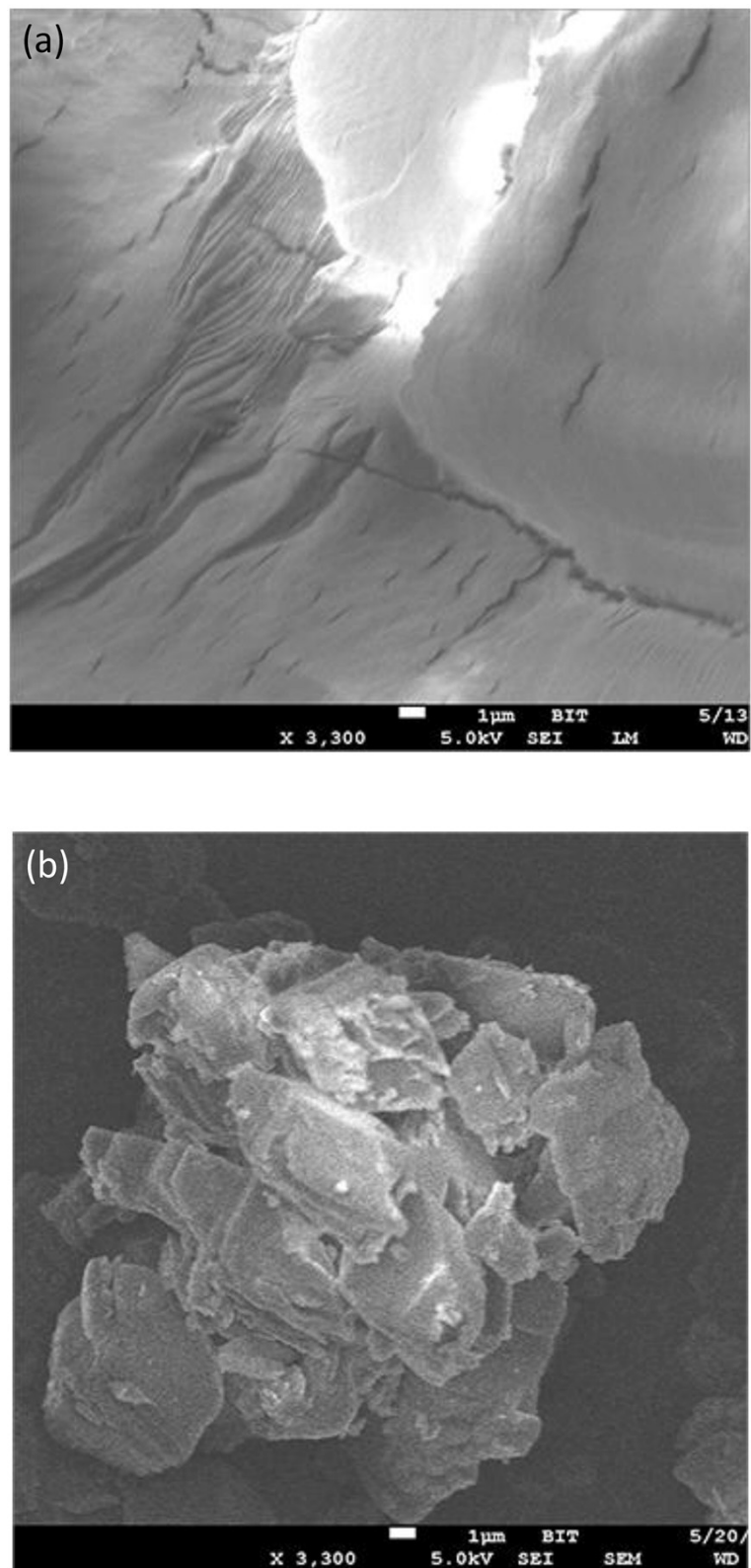


Fig. S10 Scanning electron microscope (SEM) of smashed **CIE-C** (a) and **CIE-P** (b).

12. Solid state fluorescent spectra of **CIE-C**, **CIE-P** and **CIE-Powder** soaking with different kinds of solutions

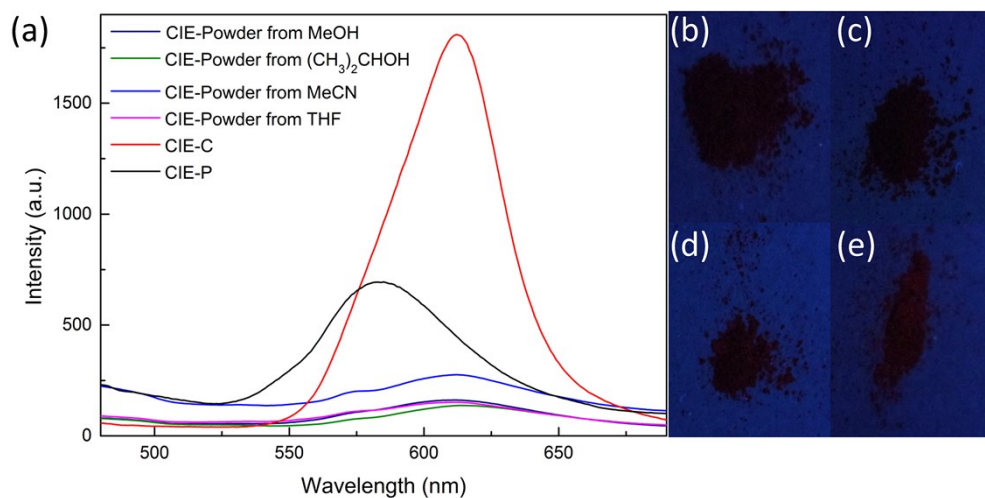


Fig. S11 Solid state fluorescent spectra of **CIE-C**, **CIE-P** and **CIE-Powder** soaking with different kinds of solutions; photographs of the solid state **CIE-Powder** from (b) MeOH, (c) $(\text{CH}_3)_2\text{CHOH}$, (d) MeCN and (e) THF under a 365 nm UV lamp excitation.

13. X-ray powder diffraction of **CIE-C**, **CIE-P** and **CIE-Powder** soaking with different kinds of solutions

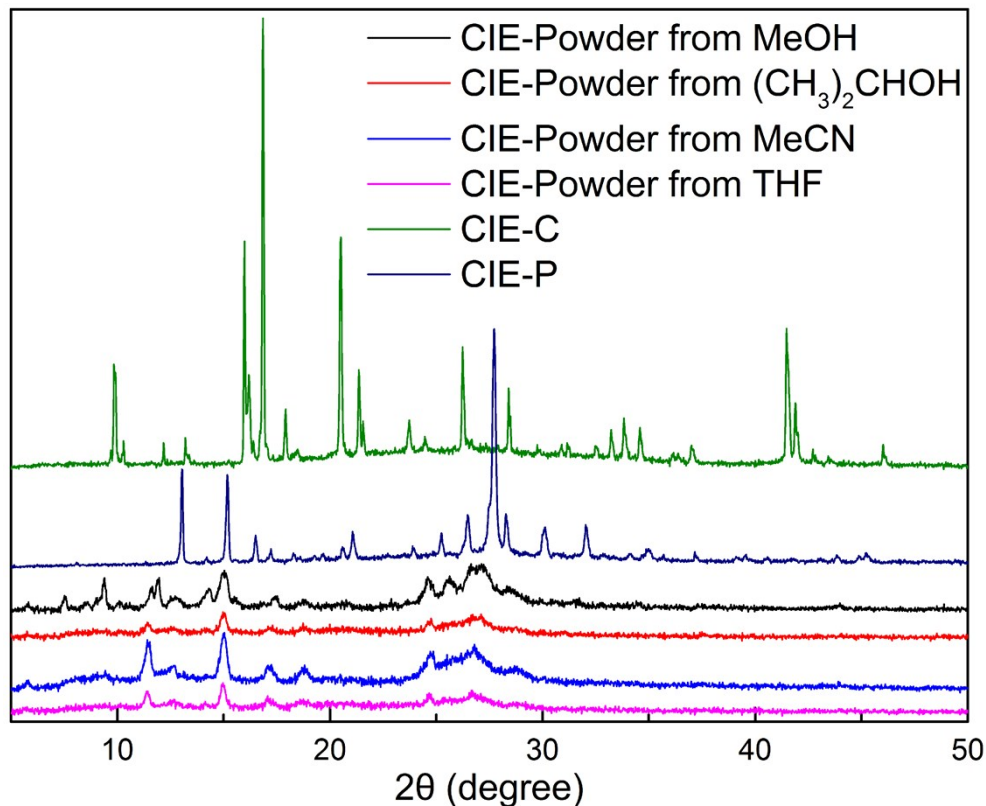


Fig. S12 PXRD of **CIE-C**, **CIE-P** and **CIE-Powder** soaking with different kinds of solutions.

14. Selected H-bonding distances of CIE-C, complexes **1** and **2**

Table S4. Selected H-bonding distances (\AA) and angles ($^\circ$) for CIE-C.

D–H	d(D–H)	d(H···A)	\angle DHA	d(D···A)	A	Symmetry
O2-H2	0.820	1.832	168.57	2.641	O3	[$x, y + 1, z$]
O1-H1A	0.866	1.833	149.41	2.616	N2	
O3-H3A	0.850	2.224	139.10	2.920	N1	

Table S5. Selected H-bonding distances (\AA) and angles ($^\circ$) for **1**.

D–H	d(D–H)	d(H···A)	\angle DHA	d(D···A)	A	Symmetry
O3-H3	0.820	1.859	167.51	2.666	O6	[$x - 1, y, z$]
O4-H4	0.820	2.023	163.74	2.820	N6	[$x - 1/2, -y + 3/2, z + 1/2$]
O6-H6	0.820	1.875	169.58	2.686	O2	[$x + 1/2, -y + 3/2, z - 1/2$]

Table S6. Selected H-bonding distances (\AA) and angles ($^\circ$) for **2**.

D–H	d(D–H)	d(H···A)	\angle DHA	d(D···A)	A	Symmetry
O3-H3	0.840	1.792	167.66	2.618	O11	[$x - 1, y, z$]
O7-H7A	0.840	1.897	171.12	2.730	N6	[$x - 1/2, -y + 1/2, z + 1/2$]
O11-H11	0.840	1.892	176.27	2.731	O1	[$x + 1/2, -y + 1/2, z - 1/2$]

15. Investigation of AIE property of CIE-C

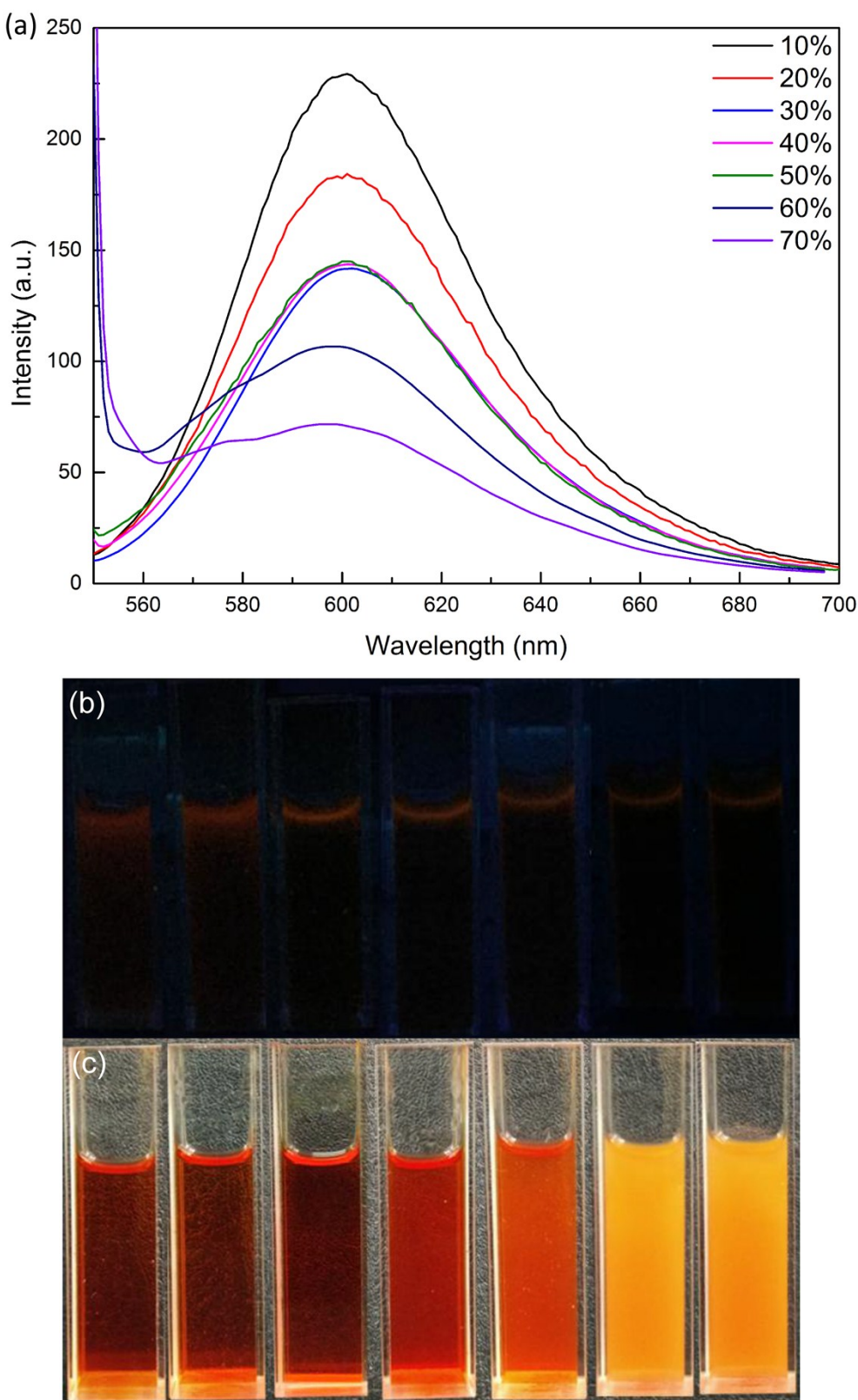


Fig. S13 (a) PL spectra of **CIE-C** in 10^{-5} M methanol/water mixture solution with different fractions (water fractions from 10% - 70%); Photos of **CIE-C** in 10^{-5} M ethanol/water mixture solution with different fractions at ultraviolet light (b) and sunlight (c) respectively.

16. Bar graph of solid state maximum fluorescent spectra of **CIE-C**, **CIE-P**, complexes **1** and **2**

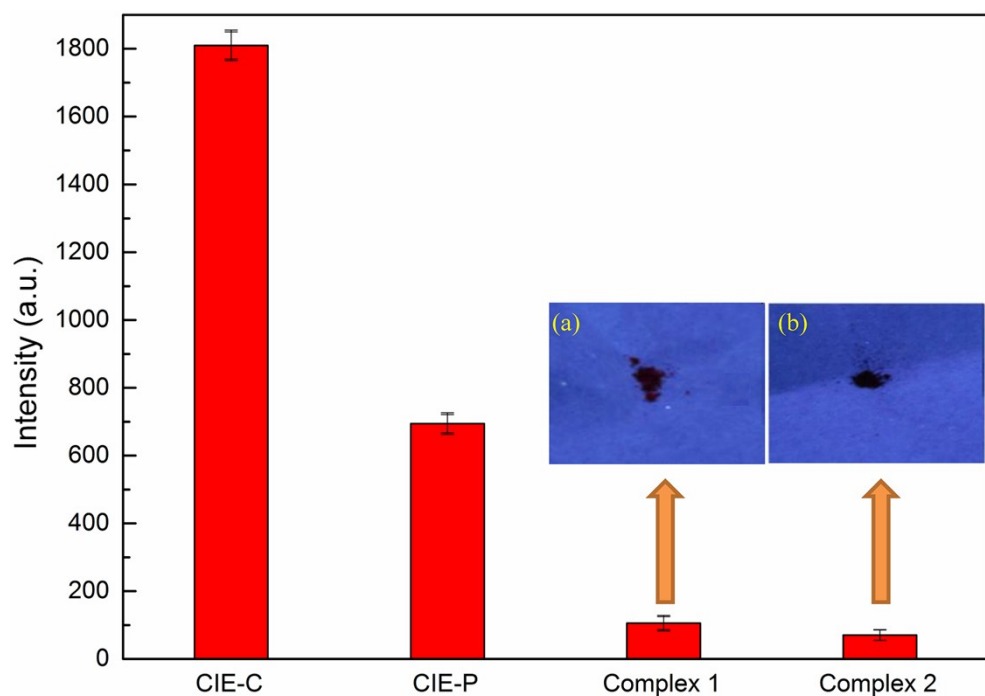


Fig. S14 Bar graph of solid state maximum fluorescent spectra of **CIE-C**, **CIE-P**, complexes **1** and **2**; Inset image (a, b) Photographs of the solid state (a) **1** and (b) **2** under a 365 nm UV lamp excitation.

17. Fluorescence spectra of **1** in different kinds of solutions and in methanol-tetrahydrofuran mixtures with different ratios.

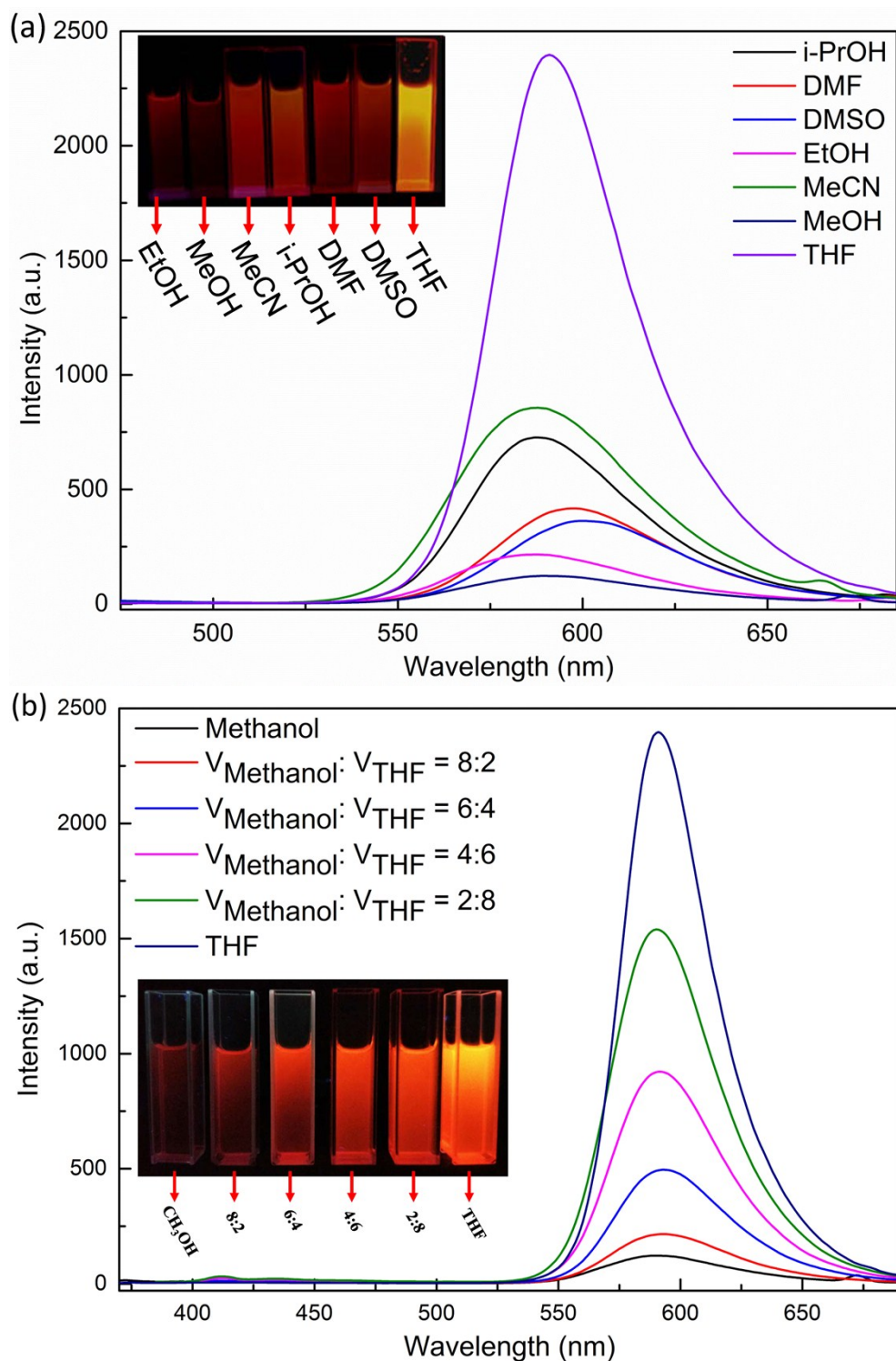


Fig. S15 (a) Fluorescence ($\lambda_{\text{exc}} = 383 \text{ nm}$) spectra of **2** ($2.5 \times 10^{-5} \text{ mol} \cdot \text{L}^{-1}$) in different solutions; Inset image: Photographs of **1** in different kinds of solutions under a 365 nm UV lamp excitation; (b) Fluorescence ($\lambda_{\text{exc}} = 384 \text{ nm}$) spectra of **1** ($2.5 \times 10^{-5} \text{ mol} \cdot \text{L}^{-1}$) in mixed solutions of methanol and tetrahydrofuran of different ratios; Inset image: Photographs of **1** ($2.5 \times 10^{-5} \text{ mol} \cdot \text{L}^{-1}$) in methanol-tetrahydrofuran mixtures with different ratios.

18. Fluorescence spectra of **2** in different kinds of solutions and in methanol-tetrahydrofuran mixtures with different ratios.

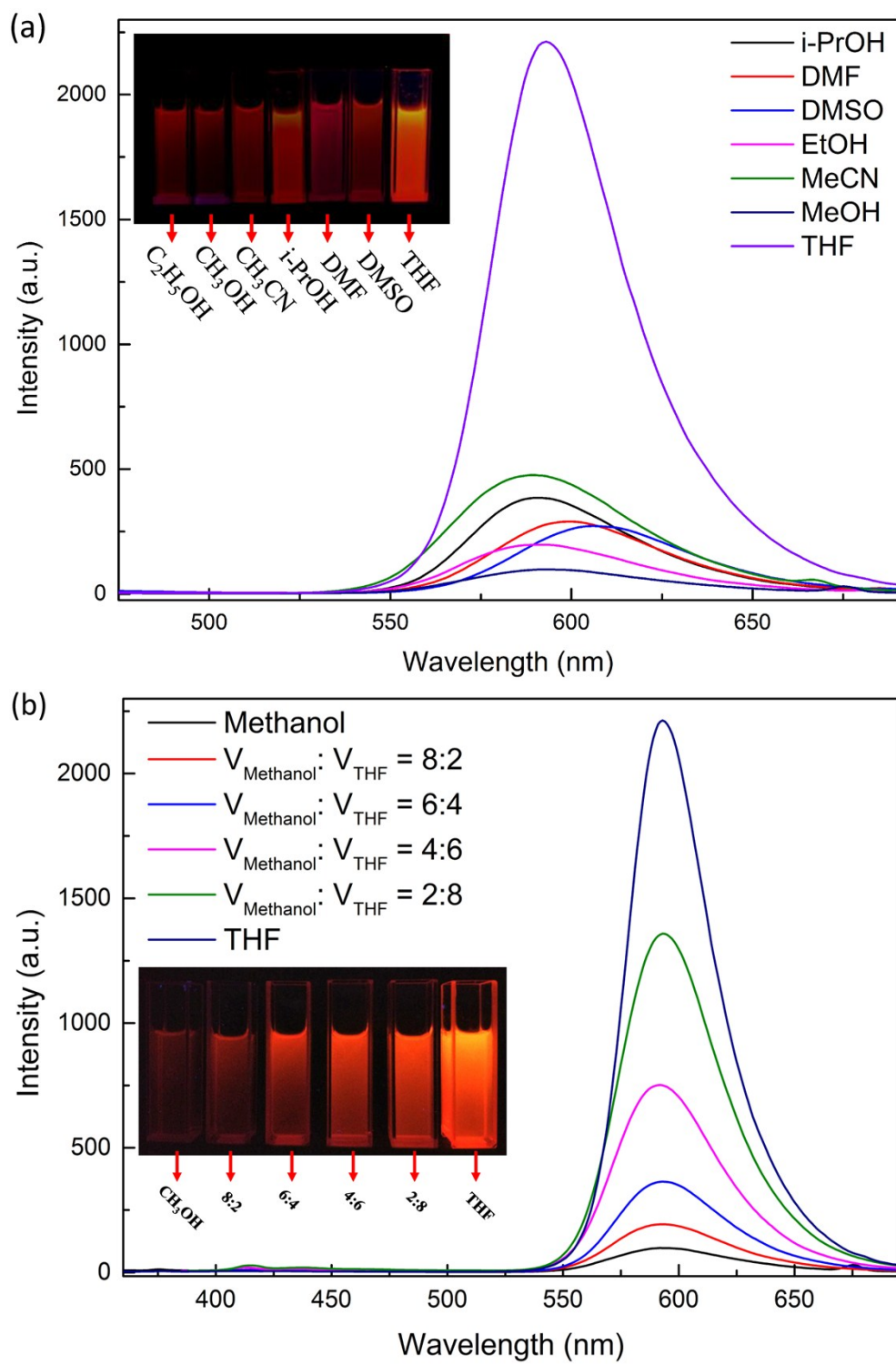


Fig. S16 (a) Fluorescence ($\lambda_{\text{exc}} = 383 \text{ nm}$) spectra of **2** ($2.5 \times 10^{-5} \text{ mol} \cdot \text{L}^{-1}$) in different solutions; Inset image: Photographs of **2** in different kinds of solutions under a 365 nm UV lamp excitation; (b) Fluorescence ($\lambda_{\text{exc}} = 384 \text{ nm}$) spectra of **2** ($2.5 \times 10^{-5} \text{ mol} \cdot \text{L}^{-1}$) in mixed solutions of methanol and tetrahydrofuran of different ratios; Inset image: Photographs of **2** ($2.5 \times 10^{-5} \text{ mol} \cdot \text{L}^{-1}$) in methanol-tetrahydrofuran mixtures with different ratios.

19. UV-Vis spectra of complexes **1** and **2** in different kinds of solutions

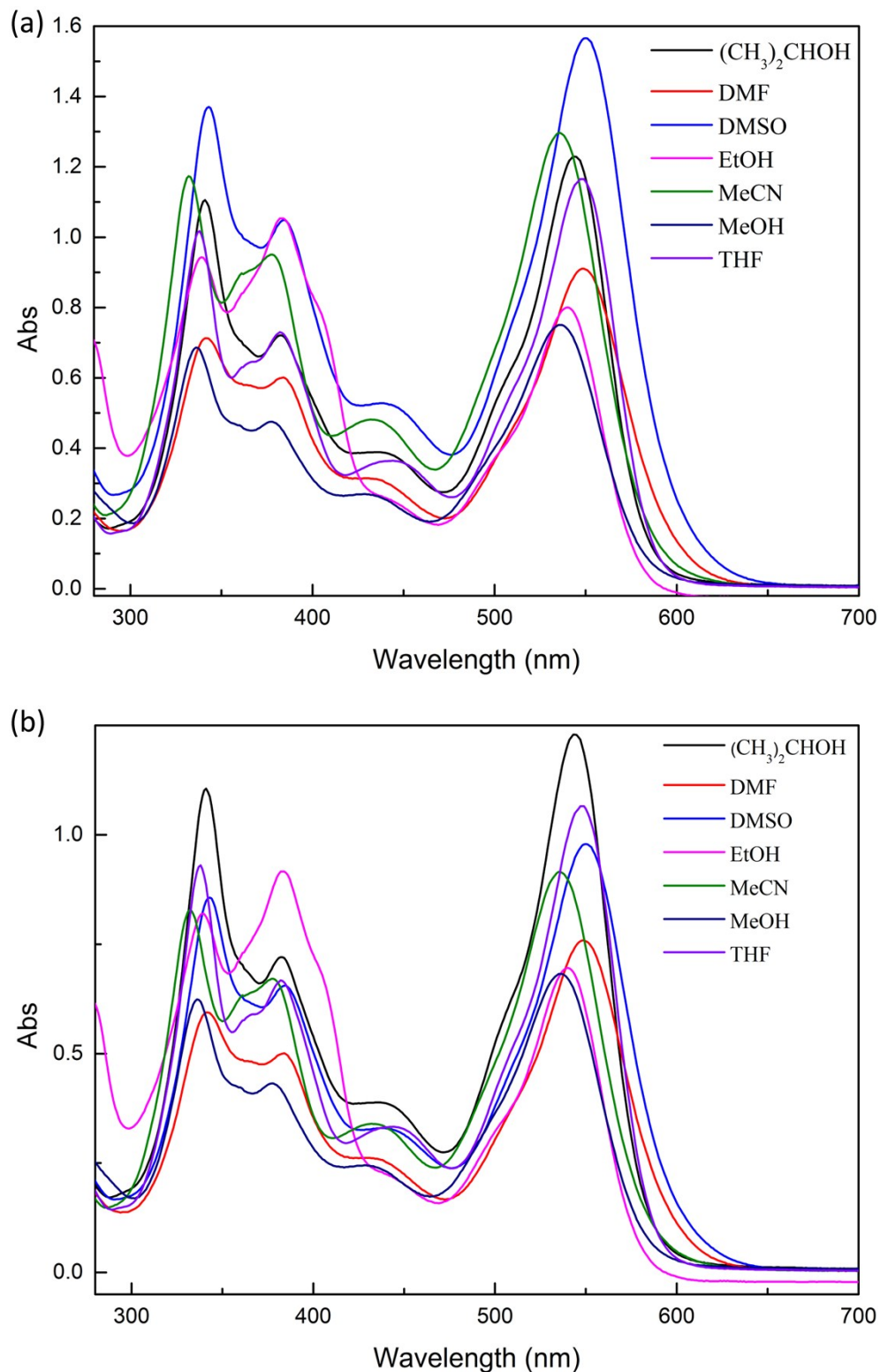


Fig. S17 UV-Vis spectra of complexes **1** ($2.5 \times 10^{-5} \text{ mol}\cdot\text{L}^{-1}$) (a) and **2** ($2.5 \times 10^{-5} \text{ mol}\cdot\text{L}^{-1}$) (b) with different solutions.

20. UV-Vis titration of complexes **1 and **2** with pyrazine and 4,4'-bipyridine**

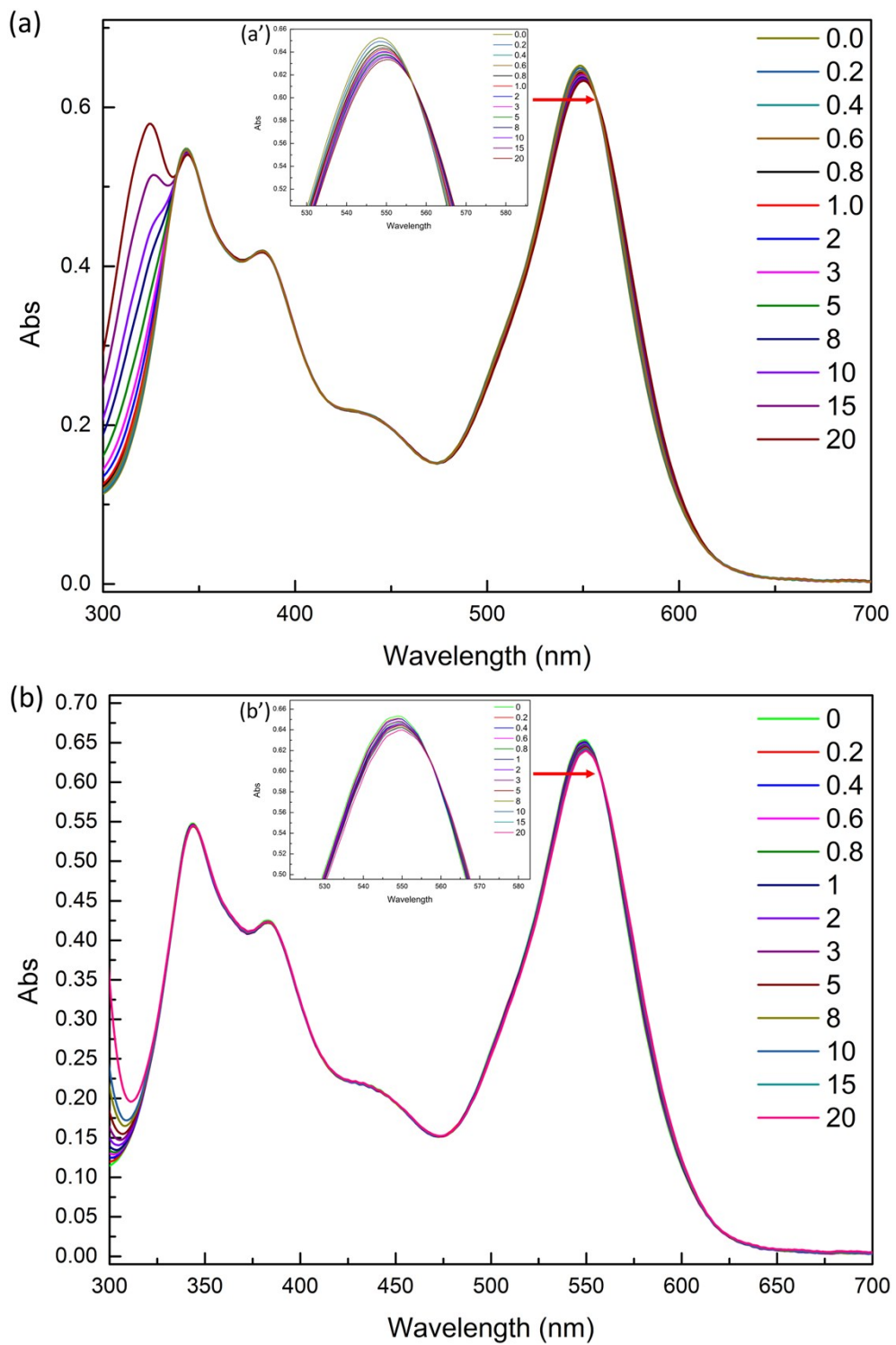


Fig. S18 UV-Vis titration spectra of Zn(II) complexes of **CIE-C** upon addition of (a) pyrazine and (b) 4,4'-bipyridine. The total concentration of these compounds in THF is held fixed (2.5×10^{-5} M) varying the ratio of the components; Inset image: Wavelength region from 520 nm to 585 nm of titration spectra of (a') Zn(II) complexes- pyrazine; (b') Zn(II) complexes- 4,4'-bipyridine.

21. Comparison of fluorescence spectra of **CIE-C**, complexes **1** and **2** in THF

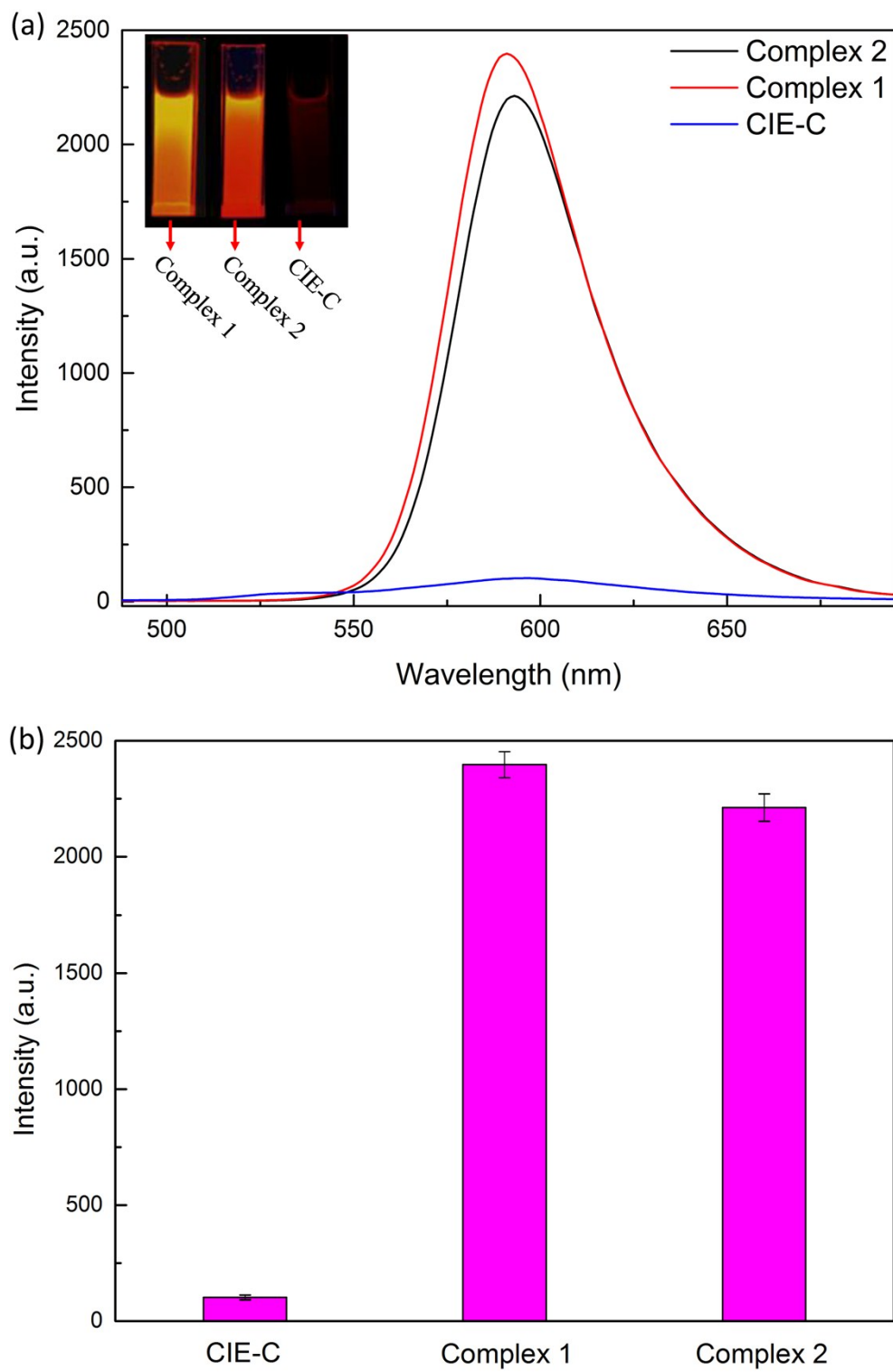


Fig. S19 (a) Fluorescence spectra ($\lambda_{\text{exc}} = 383 \text{ nm}$) of **CIE-C**, complexes **1** and **2** (concentration of every of them is $2.5 \times 10^{-5} \text{ mol} \cdot \text{L}^{-1}$) in THF; Inset image: Photographs of **CIE-C**, complexes **1** and **2** in THF under a 365 nm UV lamp excitation; (b) Bar graph of maximum fluorescent spectra ($\lambda_{\text{exc}} = 383 \text{ nm}$) of **CIE-C**, complexes **1** and **2** in THF.